Applied Catalysis B: Environmental 243 (2019) 686–692

Contents lists available at ScienceDirect

Applied Catalysis B: Environmental

journal homepage: www.elsevier.com/locate/apcatb

Photocatalytic cofactor regeneration involving triethanolamine revisited: The critical role of glycolaldehyde

Karolina Kinastowska[a], Jie Liu[b], John M. Tobin[c], Yury Rakovich[d,e,f,g], Filipe Vilela[c], Zhengtao Xu[b], Wojciech Bartkowiak[a], Marek Grzelczak[e,g,*]

[a] Department of Physical and Quantum Chemistry, Wrocław University of Science and Technology, Wybrzeże Wyspiańskiego 27, 50-370, Wrocław, Poland
[b] Department of Chemistry, City University of Hong Kong, 83 Tat Chee Avenue, Kowloon, Hong Kong, China
[c] School of Engineering and Physical Sciences, Heriot-Watt University, Edinburgh, EH14 4AS, UK
[d] Centro de Física de Materiales (MPC, CSIC-UPV/EHU), Paseo Manuel de Lardizabal 5, Donostia-San Sebastián, 20018, Spain
[e] Donostia International Physics Center, Paseo Manuel Lardizabal 4, 20018, Donostia-San Sebastián, Spain
[f] National Research Nuclear University MEPhI (Moscow Engineering Physics Institute), 31 Kashirskoe shosse, 115409 Moscow, Russian Federation
[g] Ikerbasque, Basque Foundation for Science, 48013, Bilbao, Spain

ARTICLE INFO

Keywords:
NADH photoregeneration
Cofactor
Triethanolamine
Microporous conjugated polymer
Glycolaldehyde

ABSTRACT

Triethanolamine is a widely used model electron donor that enables a fast screening of the photocatalyst parameters in both, homogeneous and heterogeneous scenarios. We report a new role of triethanolamine in heterogeneous photoregeneration of cofactor molecules – nicotinamide adenine dinucleotide (NADH) – using state-of-the-art heterogeneous photocatalysts. In contrast to the common model involving the light-induced electrons and holes generation to reduce the substrate and oxidize triethanolamine simultaneously, we identified glycolaldehyde as a stable product of triethanolamine degradation capable of reducing NAD^+. Triethanolamine, apart from playing a role of a precursor for reducing agent, maintains the alkalinity of the solution to drive the reduction. Our findings offer a fresh insight into the triethanolamine-assisted photocatalysis because glycolaldehyde as such have generally been neglected in mechanistic considerations. Moreover, a spatial and temporal decoupling of the photocatalyst from the substrate reduction reaction minimizes the product re-oxidation, thus implying a relevant feature for the real-world applications using a continuous flow setting.

1. Introduction

Back in 1978 Grätzel and coworkers have proposed the tertiary aliphatic amine (triethanolamine, TEOA) as an electron donor in their pioneering works on photocatalytic hydrogen evolution reaction [1]. Since then, TEOA has developed to become a flagship electron donor in the field of homogeneous photocatalysis [2–8]. The chemistry behind TEOA oxidation comprises a non-trivial multistep process that depends on the experimental conditions and involves the generation of positively charged aminyl radical that undergoes deprotonation to form a carbon-centered radical that eventually decomposes to glycolaldehyde (GA) and diethanolamine (DEAO) [1,9,10]. The mechanistic understanding of TOEA oxidation in homogeneous systems stimulated the use of this sacrificial agent in the heterogeneous hydrogen evolution from water [11] or reduction of CO_2 [12].

Interestingly, TEOA has also been extensively applied in photobiocatalytic processes such as non-enzymatic regeneration of cofactor molecules [13–28] (*e.g.,* NADH) using chemical, [29,30] electro- [31–36] and photochemical approaches [13–16,18–20,25,27,28,37–43]. The focus has been drawn on the photocatalysts development to increase the efficiency of cofactor photoregeneration, as it dependents on electronic properties of the material (*e.g.,* band gap energy) and the surface reaction sites that control the energy flow under the action of light. The list of suitable photocatalysts is relatively long and includes inorganic semiconductors [44], organic dyes [13], polymers [14], and plasmonic nanoparticles [15,27,28]. Virtually all the proposed photocatalysts follow the standard photoregeneration pathway that involves the light-induced generation of electrons and electron holes within the photocatalyst that drive the simultaneous NAD^+ reduction and TEOA oxidation on the photocatalyst surface, respectively (Fig. 1a). However, drawing particular attention to the architecture and composition of the photocatalyst might blur the whole picture of the photochemical process itself, especially the role of TEOA. Its chemical transformation in a photocatalytic mixture can substantially alter the light-induced energy flow, leading to a

* Corresponding author at: Donostia International Physics Center, Paseo Manuel Lardizabal 4, 20018, Donostia-San Sebastián, Spain.
E-mail address: marek.grzelczak@dipc.org (M. Grzelczak).

https://doi.org/10.1016/j.apcatb.2018.10.077
Received 14 August 2018; Received in revised form 8 October 2018; Accepted 29 October 2018
Available online 31 October 2018
0926-3373/

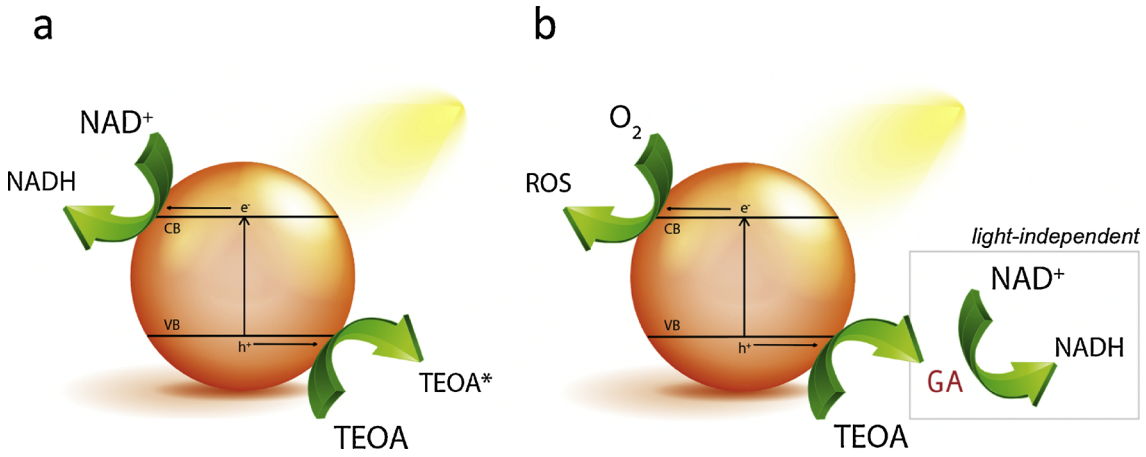

Fig. 1. Schematic illustration of cofactor (NADH) photoregeneration mechanism using semiconductor photocatalyst and TEOA as an electron donor. (a) Commonly accepted reaction route postulating simultaneous TEOA oxidation and NAD^+ reduction on the material surface (*one-pot process*). (b) Proposed alternative reaction pathway involving TEOA oxidation to glycolaldehyde - an intermediate able to reduce NAD^+ even after the light and photocatalyst removal. The molecular oxygen plays a role of an electron acceptor (*two-stage process*).

scenario unrelated to the photocatalytic mechanism in question but to the process driven by unexpectedly formed intermediates.

Herein we provide an experimental evidence that TEOA photooxidation and NAD^+ reduction are not necessarily coupled processes. We observed that the pre-irradiation of TEOA solution in the presence of state-of-the-art photocatalysts including conjugated microporous polymer [45], graphitic carbon nitride (g-C_3N_4), platinum nanoparticles (PtNP) and titanium dioxide (TiO_2) leads to the formation of glycolaldehyde, which induces NADH regeneration in the dark, even after the photocatalyst removal (Fig. 1b). We observed that NAD^+ reduction to NADH by glycolaldehyde could be suppressed by lowering the pH below 8 or by the oxygen removal from the mixture. Our findings suggest that TEOA, apart from playing a role of the chemical feedstock of an actual reducing agent (glycolaldehyde), maintains the required high pH of the mixture ensuring the reduction power of glycolaldehyde.

2. Experimental

2.1. Materials and reagents

The following were purchased from Sigma-Aldrich: TiO_2 nanopowder (< 100 nm), β-Nicotinamide adenine dinucleotide sodium salt, β-Nicotinamide adenine dinucleotide reduced disodium salt hydrate, Triethanolamine (≥99.0%), Diethanolamine (≥98.0%), Glycolaldehyde dimer, Polyvinylpyrrolidone (MW = 10k), Potassium tetrachloroplatinate (II), Sodium borohydride (ReagentPlus 99%), Sodium hydroxide, Potassium phosphate monobasic, Hydrochloric acid (37%), Perchloric acid (70%), 2,4-Dinitrophenylhydrazine, Sodium ethoxide, Benzene (99.8%). Reagents purchased from Scharlab: Ethanol (96%).

2.2. Materials synthesis

The polymer (PHTT_DMP) was synthesized as described by Tobin et al [45]. and graphitic carbon nitride was synthesized according to the procedure published by Zhang et al. [46] Polyvinylpyrrolidone (PVP) stabilized platinum nanoparticles were synthesized *via* a simple wet chemistry route at room temperature. Briefly, freshly prepared $NaBH_4$ (100 µL, 7 mM) was injected to the aqueous solution (9.9 mL) containing PVP (22 mg) and K_2PtCl_4 (1 mM). The primarily pale straw-colored solution turned grey indicating the formation of PtNP.

2.3. Materials characterization

The diffuse reflection spectra were taken with Maya2000 Pro (Ocean Optics) spectrophotometer equipped with a reflection probe (Ocean Optics, QR400-7-UV-BX) located in 6.35 mm holder using a diffuse reflectance standard (PTFE, WS-1) as a reference. Scanning electron microscopy (SEM) images were acquired using JEOL JSM-6490LV scanning electron microscope operated at accelerating voltage of 15 kV in FEI mode. Transmission electron microscopy (TEM) images were acquired using JEOL JEM-1400PLUS. The UV–vis spectra of liquid samples were collected using a scanning diode-array UV–vis spectrophotometer Agilent 8453 or JASCO V-770 UV–vis spectrophotometer. Nuclear magnetic resonance (NMR) measurements were performed with AVANCE III Bruker 500. Fluorescence lifetime measurements was done using Olympus IX71 confocal microscope system equipped by Princeton Instruments piezoscanners, 485 nm ps diode laser and single photon avalanche diode detectors (Micro Photon Devices).

2.4. Photochemical regeneration of cofactor molecules – "one-pot reaction"

All experiments were carried out using the setup consisting of a glass water-cooled mini-reactor, equipped with magnetic stirring (Fig. S1). Mili-Q water was used for preparing solutions. The reaction mixture (5 mL) containing PHTT_DMP (0.2 mg/mL), phosphate buffer (0.1 M, pH = 8), NAD^+ (1 mM) and TEOA (1 M) was incubated for 15 min in the dark. The mixture was irradiated using visible/infrared light source (MI-150TM, Dolan-Jenner Industries, 150 W) for 2 h in aerobic conditions (if not stated differently). For the spectral profile of the lamp see Fig. S2. The light power density was 230 mW/cm^2 (if not stated differently). To determine NADH regeneration kinetics, an aliquot was collected every 20 min, centrifuged and the absorbance was measured immediately (Fig. 2a). Each experiment was repeated 3 times.

2.5. Cyclic regeneration of NADH in the dark (one-pot process)

The reaction mixture (5 mL) containing PHTT_DMP (0.2 mg/mL), phosphate buffer (0.1 M, pH = 8), NAD^+ (1 mM) and TEOA (1 M) was incubated for 15 min in the dark and then irradiated for one hour with visible/infrared light (1). The polymer was removed through centrifugation and the supernatant absorbance was measured every 15 min for one hour in the dark (2). Finally, the solution was mixed back with the polymer and irradiation/incubation cycle was repeated twice (Fig. 2c).

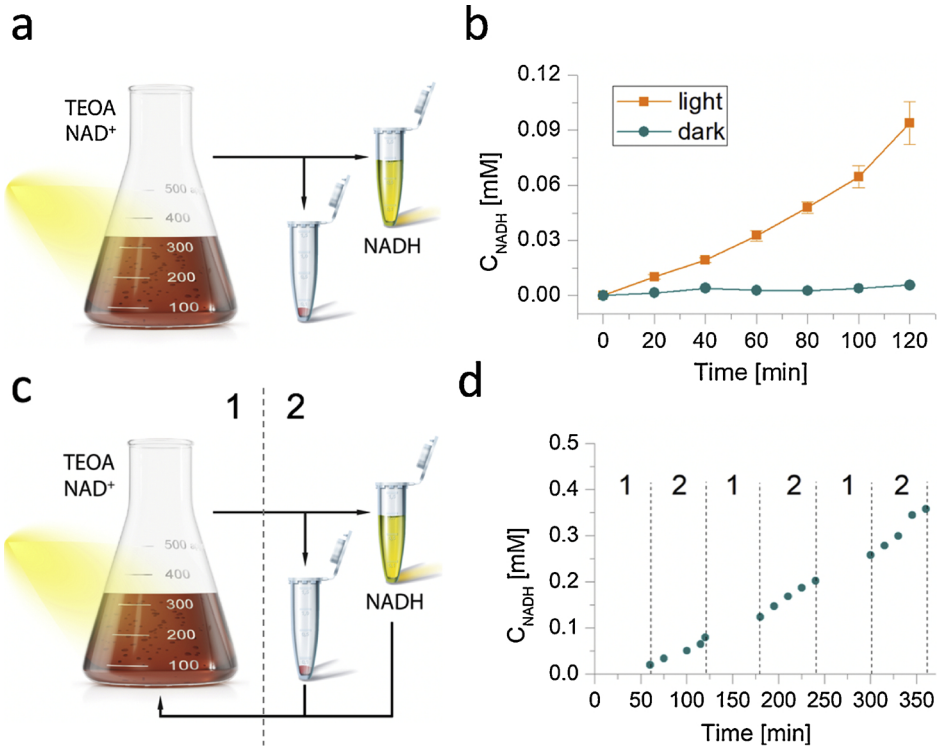

Fig. 2. Cofactor regeneration in one-pot process. (a) Typical one-pot process that involves sample irradiation for a given period of time and subsequent separation of supernatant for an immediate evaluation of NADH concentration. (b) Time-dependent NADH regeneration under irradiation (orange curve) and control experiment in which photocatalyst and cofactor is stored in the dark (green curve). (c) Scheme of alternate light and dark steps in which NADH regeneration is monitored continuously (1 h) during the dark period in the absence of polymer. After each dark step, the regenerated NADH and the polymer are combined for the subsequent light step. (d) Time-dependent NADH regeneration monitored during each dark step (2). The gaps between dark steps correspond to light steps (1). (For interpretation of the references to colour in this figure legend, the reader is referred to the web version of this article).

2.6. Regeneration of cofactor molecules in the dark – "two-stage reaction"

The reaction mixture containing the desired amount of photocatalyst (2 mg/mL), phosphate buffer (0.1 M, pH = 8) and TEOA (1 M) (or diethanolamine (DEOA), 1 M) was incubated for 15 min in the dark. The mixture was irradiated with visible / infrared light source in aerobic conditions (if not stated differently) at 230 mW/cm^2 for 2 h. In TiO_2 experiment an ultraviolet light source was used (VL-6.LC, Vilber, 6 W, λ = 365 nm). For the reaction with PtNP the irradiation time was extended to 5 h. After each reaction, the resulting solution was centrifuged to remove the photocatalyst, then 1 mM NAD^+ was added in the dark and the absorbance was monitored for 1 h (if not stated differently) (Fig. 3a).

2.7. Long-term activity of photoactivated TEOA

We investigated the long-term reducing properties of photoactivated TEOA through incubating the pre-irradiated TEOA solution (2 h irradiation in the presence of polymer) at room temperature and applying it for NAD^+ reduction in the dark at time intervals. The reducing activity decay was determined based on the NADH concentration measurements performed after an hour from NAD^+ addition.

2.8. Reduction of NAD^+ by glycolaldehyde

Three samples were prepared. These contained: I: NAD^+ (1 mM) and glycolaldehyde dimer (0.1 M); II: NAD^+ (1 mM), glycolaldehyde dimer (0.1 M) and TEOA (1 M); and III: NAD^+ (1 mM) and TEOA (1 M). The absorption spectrum of each sample was recorded after 10 min of incubation in the dark. A similar experiment was performed to evaluate the pH influence on the rate of NAD^+ reduction by GA. A set of samples containing NAD^+ (1 mM) and glycolaldehyde dimer (0.1 M) with varying pH (between 8 and 12) was prepared using NaOH as the base. The absorption spectrum of each sample was recorded after 10 min incubation in the dark. A control experiment was carried out in the absence of GA, that is, NAD^+ was incubated for 10 min at the same pH values from aforementioned range.

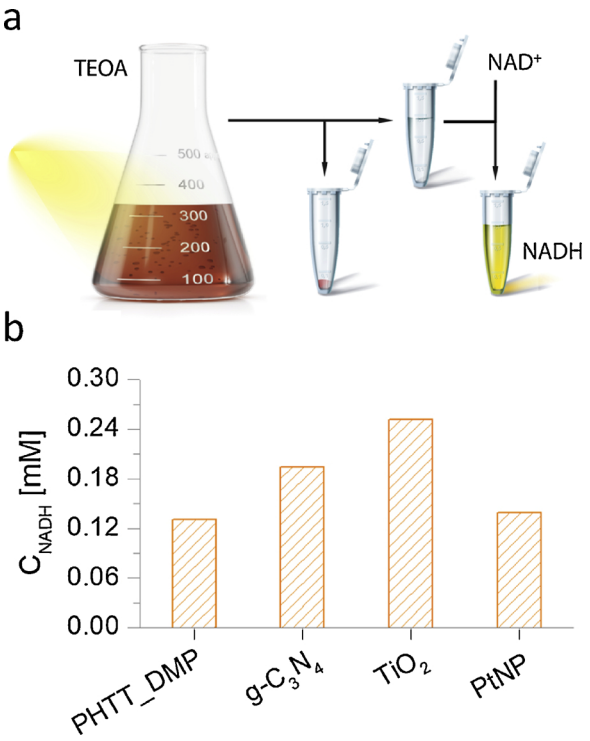

Fig. 3. Two-stage photocatalytic NADH regeneration. (a) Scheme of the experimental process: the pre-irradiated TEOA is separated from the photocatalyst followed by addition of NAD^+ for subsequent evaluation. (b) NADH regenerated in a two-step process using various photocatalysts: polymeric semiconductors, PHTT_DMP and graphitic carbon nitride using visible light (2 h irradiation), inorganic semiconductor - TiO_2 using UV light (365 nm) and platinum nanoparticles using visible light (5 h irradiation).

2.9. Inhibition of NAD^+ reduction

In a typical two-stage process, NAD^+ (1 mM) was added to two different solutions containing pre-irradiated TEOA. After 20 min of incubation the pH of one of the samples was decreased to 7.5 by HCl addition (0.92 M). In contrast, the same volume of water was added for the control sample. Absorbance measurements were continued for another 40 min and the absorbance values were recalculated taking into account the dilution factor.

2.10. NADH regeneration in anaerobic conditions

Prior to the start of the reaction, oxygen was removed from the mixture through nitrogen bubbling for 15 min. For another 15 min, N_2 was flown through the reactor in order to remove oxygen from the gas phase above the reaction mixture. The reactor was then closed and the reaction mixture was irradiated.

2.11. NMR samples preparation

The sample containing TEOA (1 M), g-C_3N_4 (2 mg/mL) and phosphate buffer (0.1 M) was irradiated for 6 h and centrifuged to remove the polymer followed by NMR measurement. Two control samples were measured: TEOA (1 M) in buffer (0.1 M) and GA (0.1 M).

3. Results and discussion

Although our central hypothesis involving the role of glycolaldehyde in cofactor regeneration is valid for a wide range of photocatalysts (*vide infra*), for the sake of simplicity we initially conducted our study using a conjugated microporous polymer (PHTT_DMP) (Fig. S3, inset, Fig. S4). Such materials have been shown as strong candidates for numerous heterogeneous photocatalytic processes [47] including cofactor regeneration [14], reactive oxygen species production [48] and hydrogen generation [49]. Our metal-free photocatalyst possesses a relatively low band gap of ~1.9 eV, thus absorbing the light in the visible spectral range (Fig. S3).

In a typical *one-pot process*, irradiation of the mixture (spectral rage: 400–1200 nm, Fig. S2) containing TEOA, NAD^+ and the polymer leads to gradual NADH regeneration. The concentration of NADH at given irradiation time was evaluated by removing an aliquot from the mixture followed by centrifugation and UV–vis characterization of supernatant (Fig. 2a). Since NADH exhibits a characteristic absorption band at 340 nm (molar absorption coefficient 6220 $M^{-1}\,cm^{-1}$), UV–vis spectroscopy facilitates a quantitative determination of the reaction efficiency. As the peak at 340 nm could correspond to NAD dimer as well, [50] the NMR measurement of the supernatant was performed to confirm NADH formation (Fig. S5).

After two hours of irradiation, the NADH concentration reached ~0.1 mM, corresponding to 10% of conversion (Fig. 2b).

Several control experiments were conducted in the one-pot reaction. We observed that increasing the polymer concentration (0–0.7 mg/mL) and light power density (0–310 mW/cm^2) lead to the increase in NADH concentration (Figs. S6, S7). The linear dependence of regenerated NADH from both parameters suggests an electron-driven chemical process with no other mechanism, such as heating involved. The requirement for both, the polymer and TEOA in cofactor regeneration was confirmed by irradiation (2 h) of the mixture containing NAD^+ with either TEOA or the polymer, in both cases resulting in no NADH formation (Fig. S8).

To our surprise, NADH regeneration continued in the dark. To evaluate the kinetics of this process, we alternated light and dark stages: after one-hour exposure to visible light (220 mW/cm^2) the mixture was centrifuged and the supernatant absorbance was monitored by UV–vis spectroscopy for one hour. The supernatant was then mixed with the polymer and moved back into the photoreactor to perform a subsequent cycle (Fig. 2c). Alternated light and dark stages revealed a linear increase of NADH concentration in the solution during the dark period (Fig. 2d), suggesting that TEOA undergoes the chemical transformation to produce intermediate species that are responsible for cofactor regeneration in the dark.

To exclude a potential involvement of the polymer degradation products in cofactor reduction in the dark we also used a range of other materials that had previously been proposed for photocatalytic one-pot NADH regeneration and claimed to comply with the common reaction mechanism. In doing so, we redesigned our experimental framework by implementing a *two-stage process* (Fig. 3a). Briefly, the mixture containing the photocatalyst and TEOA was irradiated either with visible or UV light (depending on the photocatalyst), followed by the photocatalyst removal through centrifugation or filtration and finally addition of NAD^+ to the pre-irradiated supernatant. Along with PHTT_DMP, we tested graphitic carbon nitride as an example of another semiconductor polymer, commercially available TiO_2 nanopowder (10 nm) as a conventional semiconductor oxide, and polyvinylpyrrolidone-stabilized Pt nanoparticles (1.7 ± 0.8 nm, Figs. S9, S10). Fig. 3b shows that NAD^+ indeed undergoes reduction regardless of the photocatalyst used in the pre-irradiation step, suggesting again that TEOA is a feasible source of the active species in cofactor regeneration process.

Next, we performed a series of experiments in which we modulated TEOA concentration and irradiation time in the *two-stage process*. With the increase of TEOA concentration from 0 to 1 M, the amount of NADH one hour after NAD^+ addition increased linearly to reach 15% conversion (Fig. S11). A similar linear NADH evolution was observed with the increase of irradiation time from 0 to 120 min, showing an increase of initial reduction rate from 0.02 to 2.27 μM/min, respectively (Fig. S12). Prolonged irradiation of 120 min led to 100% NADH regeneration (0.1 mM). These experiments confirm that the reactive species responsible for NAD^+ reduction arise from TEOA 'photoactivation' in the presence of the polymer. Therefore, the higher the initial TEOA concentration and irradiation time, the more reactive species produced per time unit and consequently, the higher the NADH regeneration rate.

The product of triethanolamine oxidation - glycolaldehyde is a known substrate in the enzymatic process that invovles glycolaldehyde dehydrogenase and resulting in NADH and glycolate formation [51]. Glycolaldehyde has also been shown to reduce silver ions to colloidal silver [52] and Au (III) to Au (I) in the two-electron process [53] being oxidized to glyoxal or glycolic acid [54]. Following this reasoning, we hypothesized that the holes generated within the valence band of our photocatalyst oxidize TEOA molecules leading to production of GA that subsequently oxidizes to glyoxal or glycolic acid in the light-independent process donating electrons to NAD^+ to form NADH.

To test our central hypothesis, we performed experiments with the use of commercially available glycolaldehyde (in the absence of the photocatalyst and light). We checked the ability of GA to reduce NAD^+ molecules in the presence of TEOA. We also prepared control samples containing only NAD^+ and GA or NAD^+ and TEOA. The analysis performed after 10 min of incubation revealed the presence of NADH only in the sample containing both, TEOA and GA (Fig. 4a), confirming the role of GA as a reductant in NAD^+ regeneration.

An important observation was that the presence of 1 M TEOA in the mixture of NAD^+ and GA raised the pH to 10.5, as compared to the solution with no TEOA (pH = 8). Then we hypothesize that: *TEOA maintains the pH at which the redox potential of GA is sufficient for NAD^+ reduction*. To test this hypothesis, we examined the reduction of NAD^+ by GA at pH ranging between 8 and 12 (adjusted by NaOH). With increasing pH, the NADH concentration exhibited a sigmoidal increase to reach 100% reduction at pH = 12 (Fig. 4c). In the absence of GA no NADH regeneration took place at given reaction time, regardless of the pH. To further assess the pH role in photocatalytic NADH regeneration (two-stage process), we lowered the pH from 10.5 to 7.5 *via* the addition of concentrated HCl to the mixture containing pre-irradiated TEOA and NAD^+ which inhibited the NADH regeneration (Fig. 4d). Thus, we

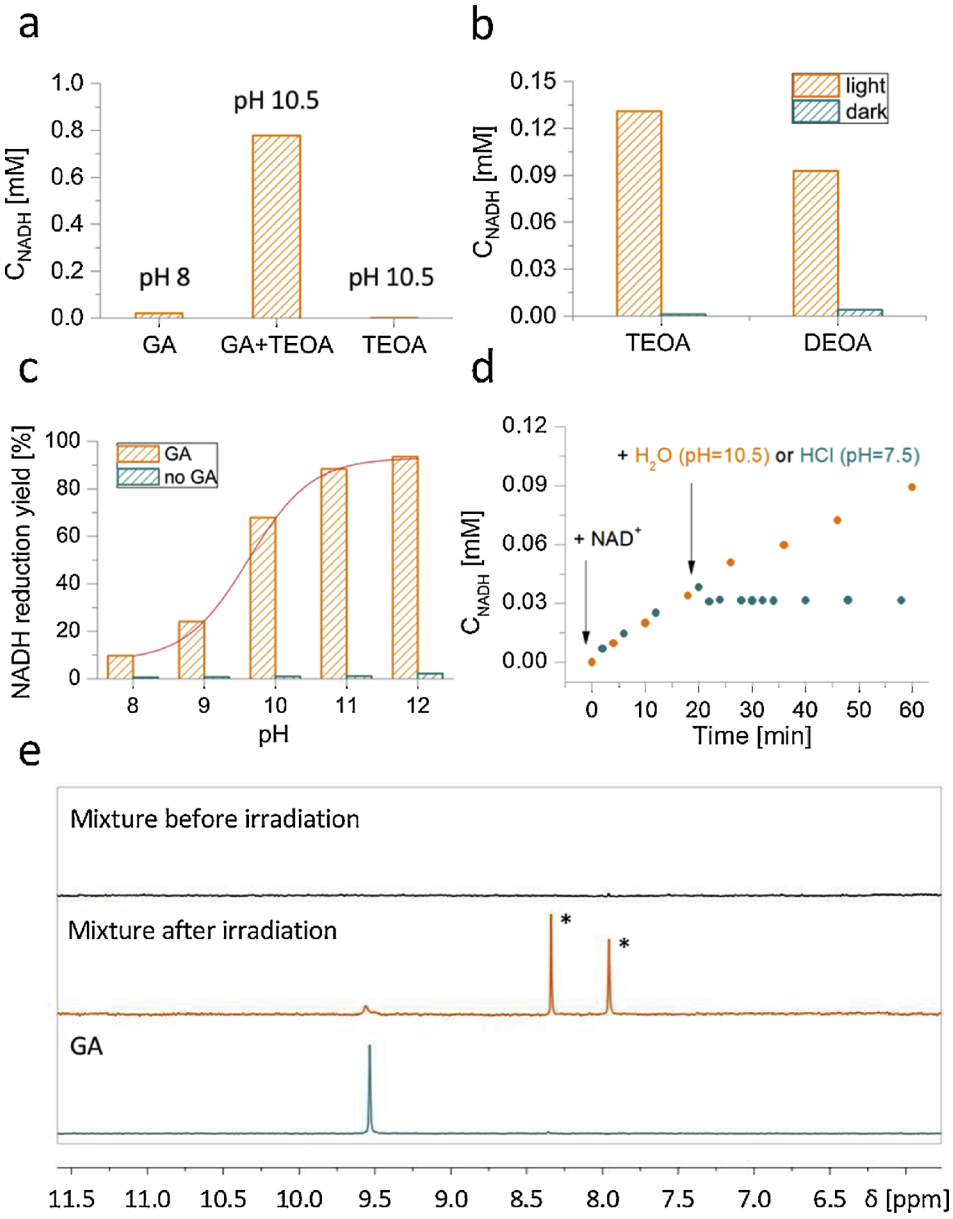

Fig. 4. Identification of glycolaldehyde as an active reducing agent. (a) Selective chemical reduction of NAD^+ in the mixture of GA and TEOA after 10 min incubation. (b) NADH photoregeneration in two-stage process using TEOA or DEOA as an electron donor. (c) Chemical reduction of NAD^+ by GA at different pH values, revealing higher effectiveness of the process in alkaline conditions. Lack of NADH in the absence of GA confirms its critical role in cofactor reduction. (d) Inhibition of NADH regeneration (two-stage process) through pH lowering. (e) NMR spectra of initial TEOA, after 6 h irradiation with g-C_3N_4 (orange curve) and pure GA in buffer. (* - aromatic products of g-C_3N_4 photodegradation) (For interpretation of the references to colour in this figure legend, the reader is referred to the web version of this article).

postulate that in our photocatalytic NADH regeneration, TEOA provides with both, the source of reducing agent (GA) and the environment alkalinity required to activate NAD^+ reduction.

Since diethanolamine is a known product of TEOA decomposition that can be oxidized to GA, we evaluated the use of diethanolamine as an electron donor in the two-step process. As expected, NAD^+ was regenerated in the presence of pre-irradiated DEOA which may indicate that GA is also a product of DEOA oxidation (Fig. 4b). In presence of DEOA, however, the NADH concentration is 30% lower as compared to TEOA. This is because the complete oxidation of one TEOA molecule can theoretically yield three molecules of GA while one DEOA molecule will yield only two GA molecules which, in turn, leads to the less effective NADH regeneration process.

The presence of GA in the pre-irradiated sample containing TEOA and the photocatalyst was confirmed by ^1H NMR measurements of the initial and irradiated TEOA solution, as well as the pure GA as a control (Fig. 4e). Since the amount of GA generated in a typical process was barely detectable, we doubled the amount of photocatalyst (g-C_3N_4) and prolonged the irradiation time to 6 h. While TEOA does not exhibit any peak in the region between 10 and 7 ppm, three new peaks occur in the spectrum of the irradiated sample. The peak located at ~9.5 ppm, also present in the pure GA spectrum, characteristic for aldehydic compounds confirms the presence of GA in the pre-irradiated mixture. The two remaining peaks located between 8.5 and 7.5 ppm (marked with stars) may indicate the formation of aromatic products of g-C_3N_4 photodegradation in the presence of TEOA.

In order to correlate the amount of generated glycolaldehyde from TEOA and amount of NADH we performed colorimetric detection GA. In doing so, the pre-irradiated mixture of TEOA was exposed to both, NAD^+ and a colorimetric assay (for details see SI – Fig. S13). We observed that pre-irradiation of 1 M TEOA gives ~100 μM of GA, while exposing the same solution to NAD^+ leads to the formation of ~300 μM of NADH. Bearing in mind the fact that regeneration of NAD^+ is a two-electron process, the 1:3 mole ratio suggests the donation of 6 electrons by each GA molecule. This may indicate that GA undergoes a multi-electron oxidation to oxalic acid (through glyoxal and glyoxylic acid) [54] loosing 2 electrons on each reaction step, thus providing with 6 electrons per 1 GA molecule.

The remaining question is the identity of the real electron acceptor during the photochemical TOEA degradation. Skrabalak et al. [52] have

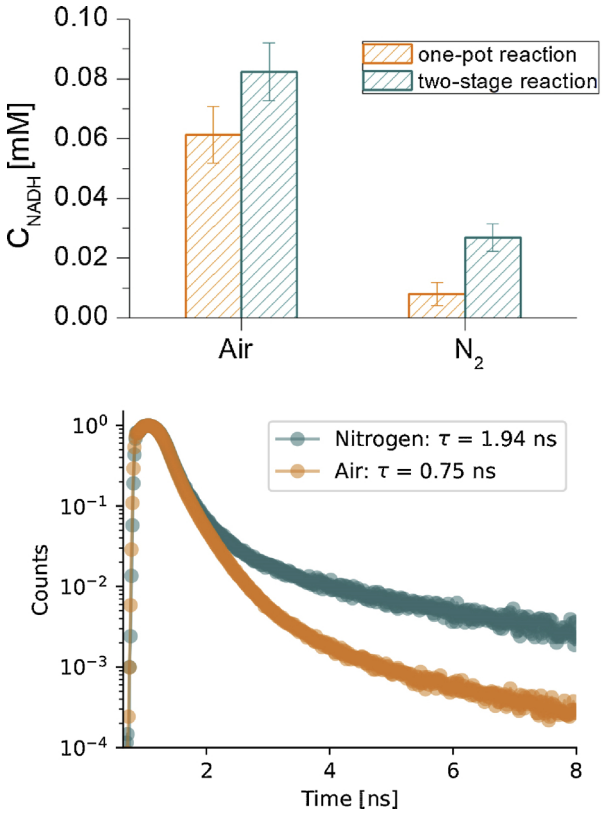

Fig. 5. Oxygen as an electron donor in photocatalytic glycolaldehyde formation. (upper) Comparison of the reaction efficiency obtained in one-pot and two-stage reactions in both, aerobic and anaerobic conditions showing higher NADH concentrations reached in the presence of air which confirms that oxygen takes part in this. (lower) Oxygen-dependent emission decay time of PHTT_DMP in the presence of TEOA (1 M) upon excitation at 480 nm. Removal of oxygen increases the decay time.

demonstrated that thermal decomposition of ethylene glycol in the presence of oxygen leads to the formation of glycolaldehyde that is an actual reducing agent in polyol silver nanoparticles synthesis. The anaerobic conditions contribute to the limited silver nanoparticles formation while saturating the reaction mixture with O_2 increases nanoparticles concentration in the final mixture. We hypothesized that oxygen can play the role of an electron acceptor also in TEOA degradation. To evaluate this statement, we compared the NADH regeneration efficiency in the presence and absence of air, in both, one-pot and two-stage modes. (Fig. 5). Although the residual amount of oxygen was present in the mixture after bubbling it with N_2 for 15 min (Fig. S14), the term “anaerobic conditions “was used throughout the article for the sake of simplicity. In anaerobic conditions, the NADH concentration was nearly 8 and 3 times lower as compared to aerobic conditions for one-pot and two-stage reactions, respectively, suggesting an active role of oxygen in TEOA photooxidation. To further confirm it we measured the emission decay time of the polymer in the presence of TOEA under aerobic and anaerobic conditions observing its increase from 0.75 to 1.94 ns upon oxygen removal (Fig. 5). These results show that the polymer promotes the electron transfer from TEOA to O_2 molecules adsorbed on the material surface leading to the formation of singlet oxygen ($^1O_2$) and/or superoxide ($O_2^{\cdot -}$) in a similar fashion as described by Tobin et al. [48]

Interestingly, the cofactor concentrations obtained in the two-stage mode are higher as compared to the one-pot process. In the presence of the photocatalyst, the as-reduced NADH can be oxidized back to NAD^+ on the material surface. As a matter of fact, we showed in another control experiment that irradiating NADH only in the presence of the polymer for 1 h leads to approximately 40% decrease in NADH concentration (Fig. S15). In the two-stage process, the backward reaction is excluded since there is no contact between the polymer and the cofactor.

4. Summary

In summary, we revisited the role of triethanolamine in the photocatalytic regeneration of cofactor molecules (NADH) by showing its dual functionality: as a precursor of glycolaldehyde - the real reductor of NAD^+ and a strong base ensuring the high pH to provide the sufficient reducing power of glycolaldehyde. The chemical stability of glycolaldehyde formed in the photochemical process allowed us to develop a new experimental model that comprises two steps: pre-irradiation of TEOA in the presence of the photocatalyst and dark reduction of cofactor molecules after the photocatalyst removal. Such a spatial and temporal decoupling of redox half-reactions eliminates the issues of an eventual NADH re-oxidation on the photocatalyst surface. In addition, the pre-irradiated mixture exhibits the long-term activity demonstrated by performing NADH regeneration using the solution stored for 11 days (Fig. S16). Revealing of oxygen’s role as an electron donor in the photochemical process, conditioning the formation of glycolaldehyde, was another significant contribution. From a broader perspective, our finding shows that photoactivation of inexpensive TEOA leads to production of a valuable chemical feedstock of relevance in organic chemistry and biology. For example, glycolaldehyde is an important intermediate in formose reaction that involves the autocatalytic synthesis of biologically-relevant sugars (*e.g.* ribose) from formaldehyde as a starting material.

Acknowledgements

Authors thanks A. Sánchez-Iglesias for TEM characterization and L. Salassa for assistance with NMR measurements. F. V. would like to thank ScotChem for the financial support. Y. R. would like to thank The Ministry of Education and Science of the Russian Federation (grant no. 14.Y26.31.0011)

Appendix A. Supplementary data

Supplementary material related to this article can be found, in the online version, at doi:https://doi.org/10.1016/j.apcatb.2018.10.077.

References

[1] K. Kalyanasundaram, J. Kiwi, M. Grätzel, Hydrogen evolution from water by visible light, a homogeneous three component test system for redox catalysis, Helv. Chim. Acta 61 (1978) 2720–2730, https://doi.org/10.1002/hlca.19780610740.
[2] M. Kirch, J.-M. Lehn, J.-P. Sauvage, Hydrogen generation by visible light irradiation of aqueous solutions of metal complexes. An approach to the photochemical conversion and storage of solar energy, Helv. Chim. Acta 62 (1979) 1345–1384, https://doi.org/10.1002/hlca.19790620449.
[3] J.-M. Lehn, R. Ziessel, Photochemical generation of carbon monoxide and hydrogen by reduction of carbon dioxide and water under visible light irradiation, Proc. Natl. Acad. Sci. 79 (1982) 701–704, https://doi.org/10.1073/pnas.79.2.701.
[4] R. Ziessel, J. Hawecker, J.-M. Lehn, Photogeneration of carbon monoxide and of hydrogenvia simultaneous photochemical reduction of carbon dioxide and water by visible-light irradiation of organic solutions containing tris(2,2-bipyridine)ruthenium(II) and cobalt(II) species as homogeneous catalysts, Helv. Chim. Acta 69 (1986) 1065–1084, https://doi.org/10.1002/hlca.19860690514.
[5] S. Matsuoka, N. Nakashima, Efficient and selective electron mediation of cobalt complexes with cyclam and related macrocycles in the p-terphenyl-catalyzed photoreduction of CO_2, J. Am. Chem. Soc. 115 (1993) 601–609, https://doi.org/10.1021/ja00055a032.
[6] A. Rosas-Hernández, H. Junge, M. Beller, Photochemical reduction of carbon dioxide to formic acid using ruthenium(II)-based catalysts and visible light, ChemCatChem 7 (2015) 3316–3321, https://doi.org/10.1002/cctc.201500494.
[7] A. Rosas-Hernández, P.G. Alsabeh, E. Barsch, H. Junge, R. Ludwig, M. Beller, Highly active and selective photochemical reduction of CO_2 to CO using molecular-defined cyclopentadienone iron complexes, Chem. Commun. 52 (2016) 8393–8396, https://doi.org/10.1039/C6CC01671E.
[8] Y. Pellegrin, F. Odobel, Sacrificial electron donor reagents for solar fuel production,

C. R. Chim. 20 (2017) 283–295, https://doi.org/10.1016/j.crci.2015.11.026.
[9] X.-J. Yang, B. Chen, L.-Q. Zheng, L.-Z. Wu, C.-H. Tung, Highly efficient and selective photocatalytic hydrogenation of functionalized nitrobenzenes, Green Chem. 16 (2014) 1082–1086, https://doi.org/10.1039/C3GC42042F.
[10] P. Du, J. Schneider, P. Jarosz, R. Eisenberg, Photocatalytic generation of hydrogen from water using a platinum(II) terpyridyl acetylide chromophore, J. Am. Chem. Soc. 128 (2006) 7726–7727, https://doi.org/10.1021/ja0610683.
[11] X. Wang, K. Maeda, A. Thomas, K. Takanabe, G. Xin, J.M. Carlsson, K. Domen, M. Antonietti, A metal-free polymeric photocatalyst for hydrogen production from water under visible light, Nat. Mater. 8 (2009) 76–80, https://doi.org/10.1038/nmat2317.
[12] J.L. White, M.F. Baruch, J.E. Pander III, Y. Hu, I.C. Fortmeyer, J.E. Park, T. Zhang, K. Liao, J. Gu, Y. Yan, T.W. Shaw, E. Abelev, A.B. Bocarsly, Light-driven heterogeneous reduction of carbon dioxide: photocatalysts and photoelectrodes, Chem. Rev. 115 (2015) 12888–12935, https://doi.org/10.1021/acs.chemrev.5b00370.
[13] J.H. Kim, M. Lee, J.S. Lee, C.B. Park, Self-assembled light-harvesting peptide nanotubes for mimicking natural photosynthesis, Angew. Chem. Int. Ed. 51 (2012) 517–520, https://doi.org/10.1002/anie.201103244.
[14] J. Liu, M. Antonietti, Bio-inspired NADH regeneration by carbon nitride photocatalysis using diatom templates, Energy Environ. Sci. 6 (2013) 1486–1493, https://doi.org/10.1039/c3ee40696b.
[15] S.S. Bhoware, K.Y. Kim, J.A. Kim, Q. Wu, J. Kim, Photocatalytic activity of Pt nanoparticles for visible light-driven production of NADH, J. Phys. Chem. C 115 (2011) 2553–2557, https://doi.org/10.1021/jp1092652.
[16] J. Liu, R. Cazelles, Z.P. Chen, H. Zhou, A. Galarneau, M. Antonietti, The bioinspired construction of an ordered carbon nitride array for photocatalytic mediated enzymatic reduction, Phys. Chem. Chem. Phys. 16 (2014) 14699–14705, https://doi.org/10.1039/C4CP01348D.
[17] D.H. Nam, S.H. Lee, C.B. Park, CdTe, CdSe, and CdS nanocrystals for highly efficient regeneration of nicotinamide cofactor under visible light, Small 6 (2010) 922–926, https://doi.org/10.1002/smll.201000077.
[18] J. Ryu, S.H. Lee, D.H. Nam, C.B. Park, Rational design and engineering of quantum-dot-Sensitized TiO_2 nanotube arrays for artificial photosynthesis, Adv. Mater. 23 (2011) 1883–1888, https://doi.org/10.1002/adma.201004576.
[19] R.K. Yadav, J.-O. Baeg, G.H. Oh, N.-J. Park, K. Kong, J. Kim, D.W. Hwang, S.K. Biswas, A photocatalyst–enzyme coupled artificial photosynthesis system for solar energy in production of formic acid from CO_2, J. Am. Chem. Soc. 134 (2012) 11455–11461, https://doi.org/10.1021/ja3009902.
[20] J. Liu, J. Huang, H. Zhou, M. Antonietti, Uniform graphitic carbon nitride nanorod for efficient photocatalytic hydrogen evolution and sustained photoenzymatic catalysis, ACS Appl. Mater. Interfaces 6 (2014) 8434–8440, https://doi.org/10.1021/am501319v.
[21] D. Yadav, R.K. Yadav, A. Kumar, N.-J. Park, J.-O. Baeg, Functionalized graphene quantum dots as efficient visible-light photocatalysts for selective solar fuel production from CO_2, ChemCatChem 8 (2016) 3389–3393, https://doi.org/10.1002/cctc.201600905.
[22] D. Yang, H. Zou, Y. Wu, J. Shi, S. Zhang, X. Wang, P. Han, Z. Tong, Z. Jiang, Constructing quantum dots@flake graphitic carbon nitride isotype heterojunctions for enhanced visible-light-driven NADH regeneration and enzymatic hydrogenation, Ind. Eng. Chem. Res. 56 (2017) 6247–6255, https://doi.org/10.1021/acs.iecr.7b00912.
[23] S.H. Lee, J. Ryu, D.H. Nam, C.B. Park, Photoenzymatic synthesis through sustainable NADH regeneration by SiO_2-supported quantum dots, Chem. Commun. 47 (2011) 4643–4645, https://doi.org/10.1039/c0cc05246a.
[24] H.Y. Lee, J. Ryu, J.H. Kim, S.H. Lee, C.B. Park, Biocatalyzed artificial photosynthesis by hydrogen-terminated silicon nanowires, ChemSusChem 5 (2012) 2129–2132, https://doi.org/10.1002/cssc.201200251.
[25] J. Huang, M. Antonietti, J. Liu, Bio-inspired carbon nitride mesoporous spheres for artificial photosynthesis: photocatalytic cofactor regeneration for sustainable enzymatic synthesis, J. Mater. Chem. A 2 (2014) 7686–7693, https://doi.org/10.1039/C4TA00793J.
[26] J.S. Lee, S.H. Lee, J.H. Kim, C.B. Park, Artificial photosynthesis on a chip: microfluidic cofactor regeneration and photoenzymatic synthesis under visible light, Lab Chip 11 (2011) 2309, https://doi.org/10.1039/c1lc20303g.
[27] A. Sánchez-Iglesias, A. Chuvilin, M. Grzelczak, Plasmon-driven photoregeneration of cofactor molecules, Chem. Commun. 51 (2015) 5330–5333, https://doi.org/10.1039/C4CC07829B.
[28] A. Sánchez-Iglesias, J. Barroso, D.M. Solís, J.M. Taboada, F. Obelleiro, V. Pavlov, A. Chuvilin, M. Grzelczak, Plasmonic substrates comprising gold nanostars efficiently regenerate cofactor molecules, J. Mater. Chem. A 4 (2016) 7045–7052, https://doi.org/10.1039/C6TA01770C.
[29] K.E. Taylor, J.B. Jones, Nicotinamide coenzyme regeneration by dihydropyridine and pyridinium compounds, J. Am. Chem. Soc. 98 (18) (1976) 5689–5694.
[30] J.B. Jones, D.W. Sneddon, Preparative-scale reductions of cyclic ketone and aldehyde substrates of horse liver alcohol dehydrogenase with in situ sodium dithionite recycling of catalytic amounts of NAD, J. Chem. Soc. Chem. Commun. 15 (1972) 856–857.
[31] E. Siu, K. Won, C.B. Park, Electrochemical regeneration of NADH using conductive vanadia-silica xerogels, Biotechnol. Prog. 23 (2007) 293–296, https://doi.org/10.1021/bp060247l.
[32] I. Ali, B. Soomro, S. Omanovic, Electrochemical regeneration of NADH on a glassy carbon electrode surface: the influence of electrolysis potential, Electrochem. Commun. 13 (2011) 562–565, https://doi.org/10.1016/j.elecom.2011.03.010.
[33] I. Ali, A. Gill, S. Omanovic, Direct electrochemical regeneration of the enzymatic cofactor 1,4-NADH employing nano-patterned glassy carbon/Pt and glassy carbon/Ni electrodes, Chem. Eng. J. 188 (2012) 173–180, https://doi.org/10.1016/j.cej.2012.02.005.
[34] I. Ali, T. Khan, S. Omanovic, Direct electrochemical regeneration of the cofactor NADH on bare Ti, Ni, Co and Cd electrodes: the influence of electrode potential and electrode material, J. Mol. Catal. Chem. 387 (2014) 86–91, https://doi.org/10.1016/j.molcata.2014.02.029.
[35] A. Damian, K. Maloo, S. Omanovic, Direct electrochemical regeneration of NADH on Au, Cu and Pt-Au electrodes, Chem. Biochem. Eng. Q. 21 (2007) 21–32.
[36] N. Ullah, I. Ali, S. Omanovic, Direct electrocatalytic reduction of coenzyme NAD+ to enzymatically-active 1,4-NADH employing an iridium/ruthenium-oxide electrode, Mater. Chem. Phys. 149–150 (2015) 413–417, https://doi.org/10.1016/j.matchemphys.2014.10.038.
[37] D.H. Nam, C.B. Park, Visible light-driven NADH regeneration sensitized by proflavine for biocatalysis, ChemBioChem 13 (2012) 1278–1282, https://doi.org/10.1002/cbic.201200115.
[38] R.K. Yadav, G.H. Oh, N.-J. Park, A. Kumar, K. Kong, J.-O. Baeg, Highly selective solar-driven methanol from CO_2 by a photocatalyst/biocatalyst integrated system, J. Am. Chem. Soc. 136 (2014) 16728–16731, https://doi.org/10.1021/ja509650r.
[39] K.T. Oppelt, E. Wöß, M. Stiftinger, W. Schöfberger, W. Buchberger, G. Knör, Photocatalytic reduction of artificial and natural nucleotide co-factors with a chlorophyll-like tin-dihydroporphyrin sensitizer, Inorg. Chem. 52 (2013) 11910–11922, https://doi.org/10.1021/ic401611v.
[40] J. Schneider, M. Matsuoka, M. Takeuchi, J. Zhang, Y. Horiuchi, M. Anpo, D.W. Bahnemann, Understanding TiO_2 photocatalysis: mechanisms and materials, Chem. Rev. 114 (2014) 9919–9986, https://doi.org/10.1021/cr5001892.
[41] A. Dibenedetto, P. Stufano, W. Macyk, T. Baran, C. Fragale, M. Costa, M. Aresta, Hybrid technologies for an enhanced carbon recycling based on the enzymatic reduction of CO2 to methanol in water: chemical and photochemical NADH regeneration, ChemSusChem 5 (2012) 373–378, https://doi.org/10.1002/cssc.201100484.
[42] K.A. Brown, M.B. Wilker, M. Boehm, H. Hamby, G. Dukovic, P.W. King, Photocatalytic regeneration of nicotinamide cofactors by quantum dot–enzyme biohybrid complexes, ACS Catal. 6 (2016) 2201–2204, https://doi.org/10.1021/acscatal.5b02850.
[43] X. Wang, H.H.P. Yiu, Heterogeneous catalysis mediated cofactor NADH regeneration for enzymatic reduction, ACS Catal. 6 (2016) 1880–1886, https://doi.org/10.1021/acscatal.5b02820.
[44] Z. Jiang, C. Lü, H. Wu, Photoregeneration of NADH using carbon-containing TiO_2, Ind. Eng. Chem. Res. 44 (2005) 4165–4170, https://doi.org/10.1021/ie049155w.
[45] J.M. Tobin, J. Liu, H. Hayes, M. Demleitner, D. Ellis, V. Arrighi, Z. Xu, F. Vilela, BODIPY-based conjugated microporous polymers as reusable heterogeneous photosensitisers in a photochemical flow reactor, Polym. Chem. 7 (2016) 6662–6670, https://doi.org/10.1039/C6PY01393G.
[46] G. Zhang, J. Zhang, M. Zhang, X. Wang, Polycondensation of thiourea into carbon nitride semiconductors as visible light photocatalysts, J. Mater. Chem. 22 (2012) 8083–8091, https://doi.org/10.1039/c2jm00097k.
[47] Y.-L. Wong, J.M. Tobin, Z. Xu, F. Vilela, Conjugated porous polymers for photocatalytic applications, J. Mater. Chem. A 4 (2016) 18677–18686, https://doi.org/10.1039/C6TA07697A.
[48] J.M. Tobin, T.J.D. McCabe, A.W. Prentice, S. Holzer, G.O. Lloyd, M.J. Paterson, V. Arrighi, P.A.G. Cormack, F. Vilela, Polymer-supported photosensitizers for oxidative organic transformations in flow and under visible light irradiation, ACS Catal. 7 (2017) 4602–4612, https://doi.org/10.1021/acscatal.7b00888.
[49] G. Zhang, Z.-A. Lan, X. Wang, Conjugated polymers: catalysts for photocatalytic hydrogen evolution, Angew. Chem. Int. Ed. 55 (2016) 15712–15727, https://doi.org/10.1002/anie.201607375.
[50] W.T. Bresnahan, P.J. Elving, Spectrophotometric investigation of products formed following the initial one-electron electrochemical reduction of nicotinamide adenine dinucleotide (NAD+), BBA Gen. Subj. 678 (1981) 151–156, https://doi.org/10.1016/0304-4165(81)90200-2.
[51] D.D. Davies, The purification and properties of glycolaldehyde dehydrogenase, J. Exp. Bot. 11 (1960) 289–295, https://doi.org/10.1093/jxb/11.3.289.
[52] S.E. Skrabalak, B.J. Wiley, M. Kim, E.V. Formo, Y. Xia, On the polyol synthesis of silver nanostructures: glycolaldehyde as a reducing agent, Nano Lett. 8 (2008) 2077–2081, https://doi.org/10.1021/nl800910d.
[53] P.K. Sen, A.B. Bilkis, K.K.S. Gupta, Kinetics and mechanism of the oxidation of glycolaldehyde by tetrachloroaurate(III), Int. J. Chem. Kinet. 30 (1998) 613–619, https://doi.org/10.1002/(SICI)1097.
[54] T. Matsumoto, M. Sadakiyo, M.L. Ooi, S. Kitano, T. Yamamoto, S. Matsumura, K. Kato, T. Takeguchi, M. Yamauchi, CO_2-free power generation on an iron group nanoalloy catalyst via selective oxidation of ethylene glycol to oxalic acid in alkaline media, Sci. Rep. 4 (2015), https://doi.org/10.1038/srep05620.